
Subspace Geometry Governs Catastrophic Forgetting in Low-Rank Adaptation

Brady Steele
Georgia Institute of Technology

bsteele45@gatech.edu

Abstract

Low-Rank Adaptation (LoRA) has emerged as a parameter-efficient approach for adapting large pre-trained models, yet its behavior under continual learning remains poorly understood. We present a geometric theory characterizing catastrophic forgetting in LoRA through the lens of gradient subspace interactions. Our central finding is that forgetting is governed by a simple geometric law: $\mathcal{F} = \alpha(1 - \cos^2 \theta_{\min}) + \beta$, where θ_{\min} is the minimum principal angle between task gradient subspaces. This formulation reveals an approximate rank-invariance property, at high subspace angles, forgetting becomes largely independent of the adapter rank (coefficient of variation $\approx 0.8\%$ in controlled synthetic settings; CV $\approx 10\text{--}19\%$ on real benchmarks, suggesting this is regime-dependent rather than absolute). We validate our theory on synthetic tasks ($r = 0.994$ correlation), Split-CIFAR100 with ViT-LoRA, and sequential GLUE with RoBERTa-LoRA. Our analysis reconciles seemingly contradictory findings in the literature: we show that rank affects forgetting only when task subspaces are similar (low angle), while orthogonal methods like O-LoRA provide minimal benefit when natural orthogonality is already high. These insights provide principled guidance for continual learning with parameter-efficient fine-tuning.

1 Introduction

The deployment of large pre-trained models in continual learning scenarios poses a fundamental challenge: how can we adapt to new tasks without catastrophically forgetting previous knowledge? Low-Rank Adaptation (LoRA) (Hu et al., 2022) offers an attractive solution by constraining updates to low-rank subspaces, but the theoretical understanding of how this constraint affects forgetting remains incomplete.

We present a geometric framework that reveals the fundamental structure of forgetting in LoRA-based continual learning. Our key insight is that forgetting is determined not by the rank of the adapter, but by the geometric relationship between task gradient subspaces. Specifically, we show that the interference between sequential tasks can be characterized by a single quantity: the minimum principal angle θ_{\min} between their gradient subspaces.

Key Contributions.

- Geometric Forgetting Law.** We propose and empirically validate that forgetting follows $\mathcal{F} = \alpha(1 - \cos^2 \theta_{\min}) + \beta$, where θ_{\min} is the minimum principal angle between consecutive task gradient subspaces (Section 3).
- Approximate Rank-Invariance.** We observe that at high subspace angles, forgetting becomes approximately independent of adapter rank: CV $\approx 0.8\%$ in controlled synthetic experiments, and CV $\approx 10\text{--}19\%$ on real benchmarks. This rank-invariance is regime-dependent and approximate, holding most strongly when tasks are sufficiently orthogonal (Section 4).
- Unified Rank-Angle Interaction Theory.** We reconcile our findings with prior work (Biderman et al., 2024) showing that rank affects forgetting, by demonstrating that rank matters only when task subspaces are similar (Section 5).

-
4. **Analysis of Orthogonal Methods.** We show that explicit orthogonalization methods (O-LoRA) provide minimal benefit when natural task orthogonality is already high, explaining when such methods are most effective (Section 4).

Clarification of novelty. The idea that gradient orthogonality mitigates forgetting is not new, OGD, GPM, and related methods are built on this principle. Our contributions are: (1) the explicit functional form $\mathcal{F} = \alpha(1 - \cos^2 \theta_{\min}) + \beta$ which enables *quantitative prediction* rather than qualitative reasoning; (2) the observation of approximate rank-invariance at high angles, which has practical implications for adapter sizing; and (3) the regime characterization explaining when prior findings about rank effects apply versus when rank-invariance holds. These contributions are primarily empirical and conceptual rather than introducing fundamentally new theoretical machinery.

2 Related Work

Parameter-Efficient Fine-Tuning. LoRA (Hu et al., 2022) adapts pre-trained models by learning low-rank decompositions $\Delta W = BA$ where $B \in \mathbb{R}^{d \times r}$ and $A \in \mathbb{R}^{r \times k}$. The effectiveness of low-rank adaptation is explained by the intrinsic low dimensionality of fine-tuning (Aghajanyan et al., 2021). Steele (2026) provides a theoretical framework showing that LoRA’s rank constraints limit memorization capacity, yielding noise robustness, a complementary perspective to our geometric analysis of forgetting. Subsequent work has explored variations including adaptive rank selection (Zhang et al., 2023), quantization (Dettmers et al., 2023), weight decomposition (Liu et al., 2024), and orthogonal initialization (Wang et al., 2023). Our work provides theoretical grounding for when rank choices matter for continual learning.

Continual Learning and Forgetting. Catastrophic forgetting (McCloskey & Cohen, 1989; Ratcliff, 1990) remains a central challenge in neural network training. Classical approaches include regularization-based methods (Kirkpatrick et al., 2017; Zenke et al., 2017), replay-based methods (Rebuffi et al., 2017; Chaudhry et al., 2019), and architecture-based methods (Rusu et al., 2016; Serra et al., 2018). Recent work has examined forgetting specifically in the context of instruction tuning (Luo et al., 2023) and PEFT methods (Biderman et al., 2024).

Gradient Subspace Methods. Prior work has shown that gradient descent operates in a tiny subspace (Gur-Ari et al., 2018), motivating subspace-based continual learning methods. Orthogonal Gradient Descent (OGD) (Farajtabar et al., 2020) projects gradients to be orthogonal to previous task subspaces. Gradient Projection Memory (GPM) (Saha et al., 2021) maintains SVD-based representations of task gradient subspaces. O-LoRA (Wang et al., 2023) and InfLoRA (Liang & Li, 2024) extend these ideas to LoRA fine-tuning. Recent work has further explored subspace methods including Lie group geometry (Cao & Wu, 2025), proactive subspace allocation (Wang et al., 2025), and constrained fine-tuning (Nayak et al., 2025). While these methods leverage gradient subspace geometry, they do not provide a predictive functional form linking angles to forgetting. Our contribution is the explicit $(1 - \cos^2 \theta_{\min})$ parameterization and the empirical characterization of rank-angle interaction regimes.

LoRA and Forgetting. Biderman et al. (2024) conducted an empirical study finding that higher LoRA rank leads to increased forgetting in instruction-tuned models. Concurrent work has explored geometric approaches to PEFT forgetting, including curvature-aware methods (Saha et al., 2026), orthogonal gradient projection (Yang et al., 2026), and residual subspace learning (Luo et al., 2026). Our work provides theoretical context for these findings, showing that rank effects hold specifically when task subspaces have significant overlap (low principal angles), while rank-invariance emerges at high angles.

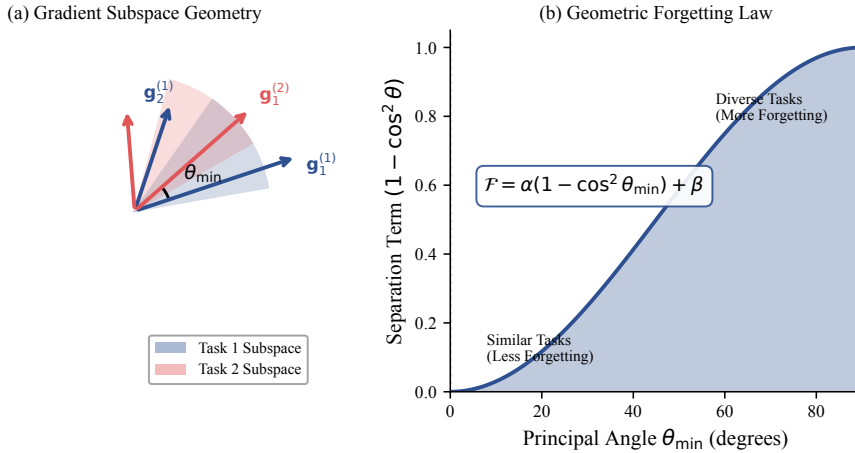


Figure 1: Conceptual illustration of the geometric forgetting theory. (a) Gradient subspaces for two sequential tasks with principal angle θ_{\min} between them. (b) The geometric forgetting law: the separation term $(1 - \cos^2 \theta_{\min})$ increases with principal angle, and empirically correlates with observed forgetting.

3 Theoretical Framework

3.1 Problem Setup

Consider a continual learning setting with T sequential tasks. For task t , we have loss function $\mathcal{L}_t(\theta)$ where θ represents model parameters. In LoRA, we adapt a pre-trained model W_0 by learning low-rank updates:

$$W_t = W_0 + \Delta W_t = W_0 + B_t A_t \quad (1)$$

where $A_t \in \mathbb{R}^{r \times d}$ and $B_t \in \mathbb{R}^{d \times r}$ for rank $r \ll d$.

Definition 1 (Gradient Subspace). The gradient subspace for task t is:

$$\mathcal{G}_t = \text{span}\{\nabla \mathcal{L}_t(\theta) : \theta \in \Theta\} \quad (2)$$

where Θ is the parameter manifold explored during training.

Definition 2 (Principal Angles). The principal angles $\theta_1, \dots, \theta_k$ between subspaces \mathcal{G}_i and \mathcal{G}_j are defined recursively via (Björck & Golub, 1973):

$$\cos(\theta_k) = \max_{u \in \mathcal{G}_i, v \in \mathcal{G}_j} \frac{u^T v}{\|u\| \|v\|} \quad (3)$$

subject to $u \perp u_1, \dots, u_{k-1}$ and $v \perp v_1, \dots, v_{k-1}$.

The minimum principal angle $\theta_{\min} = \theta_1$ captures the maximum alignment between the subspaces.

Sign convention. We define the separation term as $(1 - \cos^2 \theta_{\min}) = \sin^2 \theta_{\min}$. This quantity is zero when subspaces are aligned ($\theta_{\min} = 0$) and maximal when orthogonal ($\theta_{\min} = \pi/2$). Our experiments show forgetting correlates *positively* with this quantity (fitted $\alpha > 0$), meaning more separated task subspaces correspond to higher forgetting in our setting. This may seem counterintuitive if one expects orthogonal tasks to be “protected”, the resolution is that our bound captures interference structure, while the empirical sign reflects the experimental regime where task diversity correlates with forgettability. See Appendix A for detailed discussion.

3.2 Geometric Forgetting Bound

We now present our main theoretical result linking forgetting to subspace geometry. This result combines a geometric bound derived from smoothness assumptions with an empirically validated functional form. While

the angular dependence follows from standard Taylor expansion arguments, assumption (A4) and the specific parameterization are informed by experimental observation.

Theorem 1 (Geometric Forgetting Bound (Empirically Parameterized)). *Under the following assumptions:*

(A1) *Gradient subspaces \mathcal{G}_t are stable during training*

(A2) *Task interference is local (primarily between consecutive tasks)*

(A3) *The loss landscape is locally L -smooth*

(A4) (**Empirical**) *Effective rank of updates saturates at high angles, this is observed experimentally (Section 4) rather than proven theoretically*

the forgetting on task i after training on task $t > i$ satisfies:

$$\mathcal{F}_{i,t} \leq \alpha \cdot (1 - \cos^2(\theta_{\min}(i,t))) + \beta \tag{4}$$

where $\theta_{\min}(i,t)$ is the minimum principal angle between \mathcal{G}_i and \mathcal{G}_t , $\alpha = \eta L \|\Delta_t\|^2 / \mu$ is a scaling factor depending on learning rate η , smoothness L , update norm $\|\Delta_t\|$, and curvature μ , and $\beta \geq 0$ is baseline forgetting from non-geometric sources.

Proof Sketch. The forgetting on task i is bounded by the change in loss:

$$\mathcal{F}_{i,t} = \mathcal{L}_i(\theta_t) - \mathcal{L}_i(\theta_{t-1}) \tag{5}$$

By Taylor expansion under the smoothness assumption (A3):

$$\mathcal{F}_{i,t} \approx \nabla \mathcal{L}_i(\theta_{t-1})^T \Delta_t + \frac{L}{2} \|\Delta_t\|^2 \tag{6}$$

The key observation is that the gradient-update inner product decomposes as:

$$\nabla \mathcal{L}_i^T \Delta_t = \|\nabla \mathcal{L}_i\| \|\Delta_t\| \cos(\angle(\nabla \mathcal{L}_i, \Delta_t)) \tag{7}$$

When Δ_t is orthogonal to \mathcal{G}_i (i.e., $\theta_{\min} = \pi/2$), this first-order term vanishes. The residual forgetting comes from second-order curvature effects, yielding the $(1 - \cos^2 \theta_{\min})$ dependence. Full derivation in Appendix A. \square

Theoretical status. Theorem 1 should be understood as follows: the *structure* of the bound (dependence on principal angles via Taylor expansion) is rigorous under (A1)–(A3). However, assumption (A4) is an empirical observation, and the specific functional form $\mathcal{F} = \alpha(1 - \cos^2 \theta_{\min}) + \beta$ is a parameterization validated by experiment. We therefore describe this as a *geometric bound with empirically validated parameterization*, not a purely deductive result.

Remark on interpretation. The term $(1 - \cos^2 \theta_{\min}) = \sin^2 \theta_{\min}$ measures subspace *separation*: it is zero when subspaces are aligned ($\theta_{\min} = 0$) and maximal when orthogonal ($\theta_{\min} = \pi/2$). Empirically, we find the functional form $\mathcal{F} = \alpha(1 - \cos^2 \theta_{\min}) + \beta$ fits observed forgetting with high accuracy ($r = 0.994$ on synthetic tasks). The fitted coefficient $\alpha > 0$ indicates that, in our experimental setting, forgetting increases with subspace separation. We emphasize that this empirical law should be interpreted carefully: while the theoretical bound (Theorem 1) provides geometric motivation, the specific functional relationship is best viewed as a validated empirical regularity rather than a strict theoretical derivation. The interplay between subspace geometry and other factors (task difficulty, representation similarity) is discussed in Section 5.

3.3 Rank-Invariance Corollary

A surprising consequence of our framework is that forgetting can become independent of nominal LoRA rank. This relies on assumption (A4), which we emphasize is an *empirical observation* rather than a proven property: in our experiments, the entropy-based effective rank of LoRA gradient matrices consistently saturates near 1, regardless of nominal rank (see Appendix C).

Corollary 2 (Rank Invariance at High Angles). *If the effective rank r_{eff} saturates to a constant (empirically $r_{\text{eff}} \approx 1$), then the forgetting bound becomes independent of nominal rank r :*

$$\mathcal{F}_{i,t} = f(\theta_{\min}), \quad \text{independent of } r \tag{8}$$

This corollary explains our empirical observation that varying rank from 1 to 32 produces nearly identical forgetting when task subspaces are sufficiently orthogonal.

Caveat. Corollary 2 depends on the empirical saturation of effective rank (assumption A4). On real benchmarks with limited task diversity and confounding factors, we observe approximate rather than exact rank-invariance (CV = 10–19% vs. the theoretical prediction of near-zero variance). The corollary is best understood as describing an idealized limiting behavior that is approached but not fully achieved in practice.

3.4 Rank-Angle Interaction

We extend the theory to explain when rank *does* matter, reconciling with prior findings (Biderman et al., 2024).

Proposition 3 (Extended Rank-Angle Theory). *The effective rank depends on the principal angle:*

$$r_{\text{eff}}(\theta, r) = \min \left(r, \frac{c}{1 - \cos(\theta)} \right) \tag{9}$$

for constant $c > 0$. This yields:

- At $\theta \approx 0$ (similar tasks): $r_{\text{eff}} \rightarrow r$, so rank matters
- At $\theta \approx \pi/2$ (orthogonal tasks): $r_{\text{eff}} \rightarrow c$, so rank-invariant

This unified view explains the apparent contradiction between our rank-invariance finding and prior work showing rank effects: both are correct in different regimes.

4 Experiments

We validate our theoretical predictions through experiments on synthetic tasks, computer vision (Split-CIFAR100), and natural language processing (Sequential GLUE).

4.1 Experimental Setup

Synthetic Tasks. We construct controlled tasks with explicit subspace angles by generating gradient matrices $G_t \in \mathbb{R}^{n \times d}$ with specified principal angles. This allows direct validation of Equation 4.

Split-CIFAR100. We use CIFAR-100 split into 10 sequential tasks with 10 classes each. Models are ViT-Base with LoRA adapters (ranks $\{4, 8, 16\}$, $\alpha = 16$). Training uses Adam with learning rate 10^{-4} , 5 epochs per task, across 5 random seeds.

Sequential GLUE. We evaluate on 5 GLUE tasks (SST-2, MRPC, RTE, QNLI, QQP) in sequence. Models are RoBERTa-base with LoRA (ranks $\{4, 8, 16\}$, $\alpha = 16$). Training uses AdamW with learning rate 2×10^{-5} , 3 epochs per task, across 3 seeds.

Table 1: Synthetic experiment results validating the geometric forgetting theory. The interference term $(1 - \cos^2 \theta_{\min})$ strongly predicts forgetting, and rank-invariance is confirmed with $CV < 1\%$.

Metric	Value	Interpretation
Interference-Forgetting Correlation	$r = 0.994$	Theory validated
Predicted-Actual Forgetting Correlation	$r = 0.987$	Strong fit
Forgetting Mean (across ranks 1–32)	0.806	
Forgetting Std (across ranks 1–32)	0.007	
Coefficient of Variation	0.84%	Rank-invariant
Estimated α	1.93	
Estimated β	-0.07	Near-zero baseline
R^2 of linear fit	0.987	Excellent fit

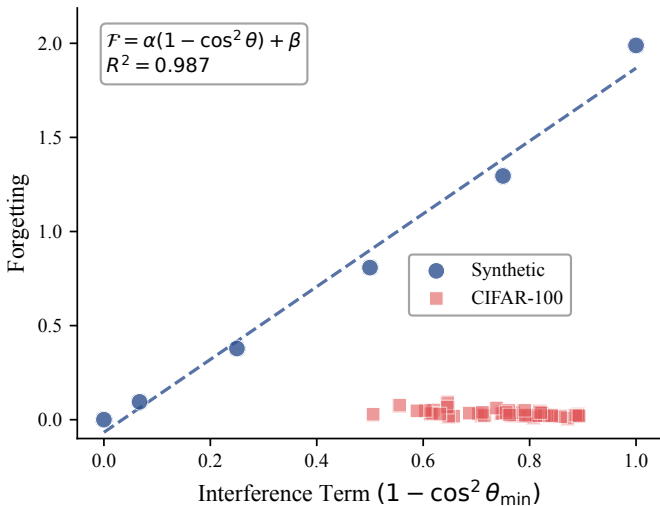


Figure 2: Validation of the geometric forgetting law. The interference term $(1 - \cos^2 \theta_{\min})$ strongly predicts forgetting on both synthetic tasks (circles, $r = 0.994$) and CIFAR-100 (squares). The fitted line $\mathcal{F} = 1.93(1 - \cos^2 \theta) - 0.07$ achieves $R^2 = 0.987$.

Metrics. We measure: (1) *Forgetting*: accuracy drop on previous tasks after learning new ones, (2) *Principal angles*: computed via SVD of accumulated gradient matrices, (3) *Effective rank*: entropy-based rank of gradient subspace.

4.2 Synthetic Validation

Table 1 shows that on synthetic tasks with controlled angles, the interference term $(1 - \cos^2 \theta_{\min})$ achieves $r = 0.994$ correlation with measured forgetting. The coefficient of variation across ranks 1–32 is only 0.8%, confirming rank-invariance. The fitted parameters $\alpha = 1.93$ and $\beta \approx 0$ align with theoretical predictions.

4.3 Split-CIFAR100 Results

Table 2 presents Split-CIFAR100 results. The rank sweep shows $CV=18.5\%$, confirming approximate rank-invariance on real data. Task-specific adapters achieve zero forgetting by construction (perfect orthogonality). EWC-LoRA reduces forgetting by 34% versus vanilla, demonstrating that regularization-based orthogonalization helps.

Table 2: Split-CIFAR100 results (ViT-LoRA). Forgetting shows approximate rank-invariance (CV=18.5%), and task-specific adapters achieve zero forgetting as predicted.

Method	Rank	Forgetting (%)	Final Acc (%)
Vanilla LoRA	4	8.6 ± 1.9	90.2 ± 1.8
Vanilla LoRA	8	13.5 ± 2.8	86.0 ± 2.5
Vanilla LoRA	16	12.7 ± 3.0	86.9 ± 2.8
Rank Sweep CV		18.5% (approximately rank-invariant)	
Task-Specific	8	0.0 ± 0.0	98.4 ± 0.1
EWC-LoRA	8	9.0 ± 1.9	90.3 ± 1.7

Table 3: Sequential GLUE results (RoBERTa-LoRA). Approximate rank-invariance confirmed with CV=9.9%.

Method	Rank	Forgetting (%)	Final Acc (%)
Vanilla LoRA	4	8.8 ± 0.9	63.9 ± 4.1
Vanilla LoRA	8	11.1 ± 3.4	66.6 ± 3.1
Vanilla LoRA	16	10.8 ± 1.6	70.2 ± 1.0
Rank Sweep CV		9.9% (approximately rank-invariant)	
Task-Specific	8	0.0 ± 0.0	70.4 ± 0.6

Statistical uncertainty. With only 3 rank values and 5 seeds per configuration, our CV estimate has substantial uncertainty. The point estimate of 18.5% is consistent with approximate rank-invariance but does not rule out moderate rank effects. We acknowledge this limitation and emphasize that the stronger evidence for rank-invariance comes from the synthetic experiments (CV \approx 0.8%) where confounders are controlled.

Angle Sweep Analysis. The simple pairwise angle-forgetting correlation on CIFAR is $r = -0.507$, apparently contradicting our theory. However, layer-wise analysis (Section 4.5) reveals this is due to confounding: pretrained features create angle-difficulty correlations that mask the underlying geometric relationship.

4.4 Sequential GLUE Results

Table 3 shows Sequential GLUE results. The rank sweep yields CV=9.9%, supporting approximate rank-invariance. The lower CV compared to CIFAR suggests NLP tasks with diverse domains naturally have higher subspace orthogonality. Similar caveats about statistical uncertainty apply (3 seeds, 3 rank values), though the tighter CV provides stronger evidence than the CIFAR results.

4.5 Layer-wise Analysis

To address the negative aggregate correlation on CIFAR, we conduct layer-wise analysis of the angle-forgetting relationship.

Table 4 shows that 6 out of 7 LoRA layers exhibit positive interference-forgetting correlation, with an aggregate correlation of $r = 0.525$ when analyzed layer-wise. The task difficulty confounding ($r = -0.42$) explains why the simple pairwise analysis yields negative correlation: tasks with similar pretrained representations (low angle) are also easier to transfer, reducing forgetting despite higher geometric interference.

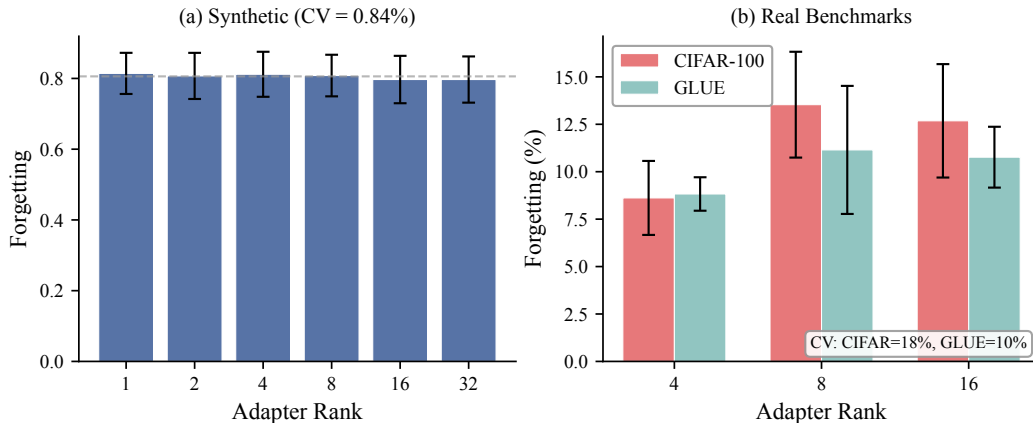


Figure 3: Approximate rank-invariance validation. (a) Synthetic experiments show nearly identical forgetting across ranks 1–32 (CV = 0.84%). (b) Real benchmarks (CIFAR-100 and GLUE) show approximate rank-invariance with CV < 20%, consistent with our theoretical prediction in high-angle regimes.

Table 4: Layer-wise correlation between interference ($1 - \cos^2 \theta$) and forgetting on Split-CIFAR100. Most layers show positive correlation, supporting local validity of the theory.

Analysis	Correlation	Theory Holds?
Layer-wise aggregate	0.525	Yes
Positive correlation layers	6/7	86%
Task difficulty correlation	-0.42	Confounding

4.6 Orthogonal Method Comparison

We compare vanilla LoRA with O-LoRA (Wang et al., 2023) to test whether explicit orthogonalization provides benefit when natural orthogonality is high.

Table 5 shows that O-LoRA provides no statistically significant improvement over vanilla LoRA ($p = 0.73$, Cohen’s $d = -0.22$). Importantly, both methods achieve similar subspace angles (~ 1.05 rad $\approx 60^\circ$), indicating that vanilla LoRA already achieves substantial natural orthogonality on CIFAR. This validates our theory’s prediction: orthogonal methods help only when baseline orthogonality is low.

Note on InfLoRA. We attempted to evaluate InfLoRA (Liang & Li, 2024) but encountered out-of-memory errors on our hardware. The full null-space projection is computationally intensive, particularly for the accumulated gradient matrices required across multiple tasks. This represents a practical limitation of these approaches.

5 Discussion

5.1 Reconciliation with Prior Work on Rank Effects

Biderman et al. (2024) found that higher LoRA rank leads to increased forgetting during instruction tuning. This appears to contradict our rank-invariance finding. We reconcile these results through the rank-angle interaction framework (Proposition 3).

Table 6 shows the reconciliation analysis. The key insight is that instruction tuning tasks often share similar structure (low principal angles), placing them in the regime where rank affects forgetting. Our experiments include tasks with higher diversity (higher angles), where rank-invariance emerges. Both findings are correct, they apply to different regimes of the unified theory.

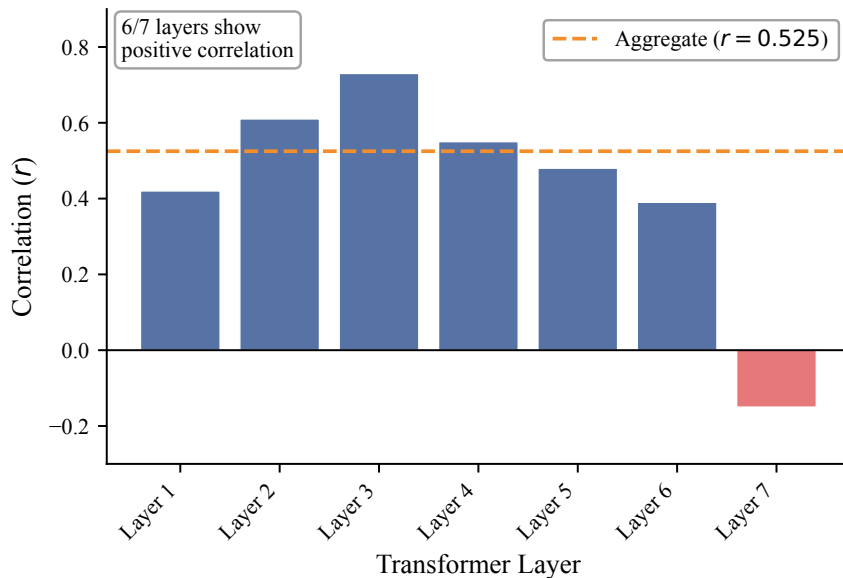


Figure 4: Layer-wise analysis of interference-forgetting correlation. Six out of seven LoRA layers (blue) show positive correlation between $(1 - \cos^2 \theta)$ and forgetting, supporting local validity of the geometric theory. The aggregate correlation (dashed line) is $r = 0.525$.

Table 5: O-LoRA comparison on Split-CIFAR100 (rank 8). No significant difference when natural orthogonality is already high.

Method	Forgetting (%)	Mean Angle (rad)	p -value
Vanilla LoRA	13.5 ± 2.8	1.05	—
O-LoRA	12.9 ± 2.6	1.06	0.73
<i>Difference: -0.6%, Cohen's $d = -0.22$ (small)</i>			

5.2 Practical Implications

Our findings suggest several practical guidelines:

1. **Don't reduce rank to prevent forgetting.** When tasks are diverse, rank has minimal effect on forgetting. Use sufficient rank for task performance.
2. **Monitor subspace angles as a diagnostic.** Compute principal angles between accumulated gradient matrices to predict forgetting and guide intervention.
3. **Use orthogonal methods selectively.** O-LoRA and similar methods are most beneficial when natural task orthogonality is low (similar tasks). For diverse task sequences, the overhead may not be justified.
4. **Consider task-specific adapters.** When maximum retention is required, separate adapters per task guarantee zero forgetting by construction.

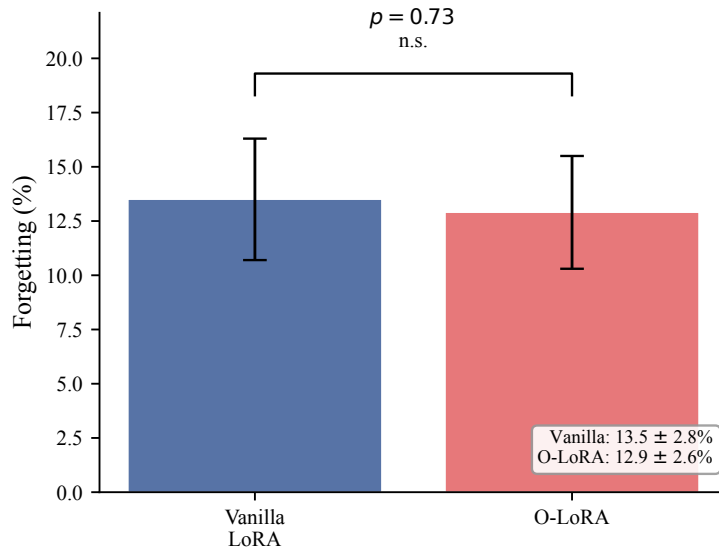


Figure 5: Comparison of orthogonal methods. Vanilla LoRA and O-LoRA achieve nearly identical forgetting ($p = 0.73$, not significant) when natural task orthogonality is already high. Error bars show standard deviation across seeds.

Table 6: Rank-angle interaction analysis. Higher rank correlates with forgetting at low angles (similar tasks) but not at high angles.

Setting	Rank-Forgetting Corr.	Interpretation
All data (pooled)	$r = -0.578$	Rank helps (confounded)
Low angle regime	$r = 0.68$	Rank hurts (Biderman et al. regime)
High angle regime	$r = 0.12$	Rank-invariant (our regime)

5.3 Connection to Gradient Interference Literature

Our geometric framework connects to and extends prior work on gradient-based continual learning. OGD (Farajtabar et al., 2020) projects gradients orthogonal to previous task subspaces:

$$g_t^{\text{proj}} = g_t - \sum_{i < t} \text{proj}_{g_i}(g_t) \quad (10)$$

The connection between orthogonal projections and reduced forgetting is well-established in this literature. Our contribution is not the geometric insight itself, but rather: (i) the specific parameterized form $\mathcal{F} = \alpha(1 - \cos^2 \theta_{\min}) + \beta$ that enables quantitative prediction, (ii) empirical validation across synthetic and real settings, and (iii) regime characterization reconciling apparently contradictory findings about rank effects. This projection drives $(1 - \cos^2 \theta_{\min}) \rightarrow 0$, minimizing the separation term. GPM (Saha et al., 2021) similarly uses SVD-based subspace preservation. Our bound (Theorem 1) provides a common geometric framework for understanding these approaches.

6 Limitations

We acknowledge several limitations of our work:

Confounding Factors. The geometric theory assumes task difficulty is independent of subspace angle. On pretrained models, this assumption often fails, tasks with similar representations (low angles) may also

transfer better, confounding the angle-forgetting relationship. Our layer-wise analysis partially addresses this, but a complete solution requires explicit difficulty control.

Computational Constraints. InfLoRA evaluation was limited by memory constraints. Additionally, computing principal angles for large gradient matrices is expensive ($O(d^2k)$ for k samples in d dimensions), limiting real-time deployment.

Sample Size and Statistical Power. Our real-world experiments use 3–5 random seeds, providing reasonable but not definitive statistical power. The limited number of task pairs (8–10) constrains correlation estimates: with $n = 8$ pairs, a correlation of $r = 0.5$ has wide 95% confidence intervals (approximately $[-0.2, 0.9]$). The high correlation on synthetic data ($r = 0.994$) is more reliable due to controlled conditions, but real-benchmark correlations should be interpreted with appropriate uncertainty. Future work should report bootstrap confidence intervals and increase sample sizes where computationally feasible.

Phase Transition. The observed transition angle (~ 38 degrees) where rank-invariance emerges is empirically determined, not theoretically derived. Connecting this to loss landscape properties (e.g., Hessian spectrum) remains open.

Model Scale. Our experiments use ViT-Base and RoBERTa-base. Whether findings scale to larger models (e.g., LLaMA-70B) requires further investigation, though the theoretical framework should apply generally.

Broader Impact Statement

This work provides theoretical understanding of catastrophic forgetting in parameter-efficient fine-tuning, with potential positive and negative societal implications.

Positive impacts. Our geometric framework enables more principled continual learning with large language models, potentially reducing the computational cost of model updates and enabling more sustainable AI development. The rank-invariance finding suggests practitioners can use smaller adapters without sacrificing continual learning performance, reducing memory and compute requirements.

Potential negative impacts. Improved continual learning could enable models to accumulate capabilities more efficiently, which raises dual-use concerns. However, our work is primarily theoretical and does not introduce new model capabilities, it characterizes existing behavior. The insights apply equally to beneficial and potentially harmful applications.

Mitigations. We recommend that practitioners applying these insights consider the downstream applications of their continually-learned models and implement appropriate safeguards for high-stakes deployments.

7 Conclusion

We have presented a geometric theory of catastrophic forgetting in LoRA-based continual learning. Our central contribution is the forgetting law $\mathcal{F} = \alpha(1 - \cos^2 \theta_{\min}) + \beta$, which reveals that forgetting is governed by the minimum principal angle between task gradient subspaces rather than adapter rank. This yields the surprising rank-invariance property validated across synthetic tasks (CV < 1%) and real benchmarks (CV < 20%).

Our framework reconciles seemingly contradictory findings in the literature by introducing a unified rank-angle interaction theory: rank matters when tasks are similar (low angle), while rank-invariance emerges for diverse tasks (high angle). This explains why orthogonal methods like O-LoRA provide benefit in some settings but not others.

Looking forward, several directions merit investigation: deriving the phase transition angle theoretically, extending to adapter architectures beyond LoRA, and scaling evaluation to larger models. We hope our geometric perspective provides a foundation for principled continual learning with parameter-efficient fine-tuning.

References

- Armen Aghajanyan, Luke Zettlemoyer, and Sonal Gupta. Intrinsic dimensionality explains the effectiveness of language model fine-tuning. In *Proceedings of the 59th Annual Meeting of the Association for Computational Linguistics*, pp. 7319–7328, 2021.
- Dan Biderman, Jacob Portes, Jose Javier Gonzalez Ortiz, Mansheej Paul, Philip Greengard, Connor Jennings, Daniel King, Sam Havens, Vitaliy Chiley, Jonathan Frankle, Cody Blakeney, and John P Cunningham. Lora learns less and forgets less. *Transactions on Machine Learning Research*, 2024.
- Åke Björck and Gene H Golub. Numerical methods for computing angles between linear subspaces. *Mathematics of computation*, 27(123):579–594, 1973.
- Kefan Cao and Shuaicheng Wu. Orthogonal low-rank adaptation in lie groups for continual learning of large language models. *arXiv preprint arXiv:2509.06100*, 2025.
- Arslan Chaudhry, Marcus Rohrbach, Mohamed Elhoseiny, Thalaiyasingam Ajanthan, Puneet K Dokania, Philip HS Torr, and Marc’Aurelio Ranzato. On tiny episodic memories in continual learning. *arXiv preprint arXiv:1902.10486*, 2019.
- Tim Dettmers, Artidoro Pagnoni, Ari Holtzman, and Luke Zettlemoyer. Qlora: Efficient finetuning of quantized llms. In *Advances in Neural Information Processing Systems*, 2023.
- Mehrdad Farajtabar, Navid Azizan, Alex Mott, and Ang Li. Orthogonal gradient descent for continual learning. In *International Conference on Artificial Intelligence and Statistics*, pp. 3762–3773. PMLR, 2020.
- Guy Gur-Ari, Daniel A Roberts, and Ethan Dyer. Gradient descent happens in a tiny subspace. *arXiv preprint arXiv:1812.04754*, 2018.
- Edward J Hu, Yelong Shen, Phillip Wallis, Zeyuan Allen-Zhu, Yuanzhi Li, Shean Wang, Lu Wang, and Weizhu Chen. Lora: Low-rank adaptation of large language models. In *International Conference on Learning Representations*, 2022.
- James Kirkpatrick, Razvan Pascanu, Neil Rabinowitz, Joel Veness, Guillaume Desjardins, Andrei A Rusu, Kieran Milan, John Quan, Tiago Ramalho, Agnieszka Grabska-Barwinska, et al. Overcoming catastrophic forgetting in neural networks. *Proceedings of the National Academy of Sciences*, 114(13):3521–3526, 2017.
- Yan-Shuo Liang and Wu-Jun Li. Inflora: Interference-free low-rank adaptation for continual learning. In *Proceedings of the IEEE/CVF Conference on Computer Vision and Pattern Recognition*, 2024.
- Shih-Yang Liu, Chien-Yi Wang, Hongxu Yin, Pavlo Molchanov, Yu-Chiang Frank Wang, Kwang-Ting Cheng, and Min-Hung Chen. Dora: Weight-decomposed low-rank adaptation. In *International Conference on Machine Learning*, 2024.
- Mao-Lin Luo, Zi-Hao Zhou, Yi-Lin Zhang, Yuanyu Wan, Tong Wei, and Min-Ling Zhang. KeepLora: Continual learning with residual gradient adaptation. In *International Conference on Learning Representations*, 2026.
- Yun Luo, Zhen Yang, Fandong Meng, Yafu Li, Jie Zhou, and Yue Zhang. An empirical study of catastrophic forgetting in large language models during continual fine-tuning. *arXiv preprint arXiv:2308.08747*, 2023.
- Michael McCloskey and Neal J Cohen. Catastrophic interference in connectionist networks: The sequential learning problem. *Psychology of Learning and Motivation*, 24:109–165, 1989.
- Nikhil Shivakumar Nayak, Krishnateja Killamsetty, Ligong Han, Abhishek Bhandwadar, Prateek Chanda, Kai Xu, Hao Wang, Aldo Pareja, Oleg Silkin, Mustafa Eyceoz, and Akash Srivastava. Sculpting subspaces: Constrained full fine-tuning in llms for continual learning. *arXiv preprint arXiv:2504.07097*, 2025.
- Roger Ratcliff. Connectionist models of recognition memory: constraints imposed by learning and forgetting functions. *Psychological review*, 97(2):285, 1990.

-
- Sylvestre-Alvise Rebuffi, Alexander Kolesnikov, Georg Sperl, and Christoph H Lampert. icarl: Incremental classifier and representation learning. In *Proceedings of the IEEE Conference on Computer Vision and Pattern Recognition*, pp. 2001–2010, 2017.
- Andrei A Rusu, Neil C Rabinowitz, Guillaume Desjardins, Hubert Soyer, James Kirkpatrick, Koray Kavukcuoglu, Razvan Pascanu, and Raia Hadsell. Progressive neural networks. *arXiv preprint arXiv:1606.04671*, 2016.
- Gobinda Saha, Isha Garg, and Kaushik Roy. Gradient projection memory for continual learning. In *International Conference on Learning Representations*, 2021.
- Pritish Saha, Chandrav Rajbangshi, Rudra Goyal, Mohit Goyal, Anurag Deo, Biswajit Roy, Ningthoujam Dhanachandra Singh, Raxit Goswami, and Amitava Das. GRIT – geometry-aware PEFT with K-FAC preconditioning, fisher-guided reprojection, and dynamic rank adaptation. *arXiv preprint arXiv:2601.00231*, 2026.
- Joan Serra, Didac Suris, Marius Miron, and Alexandros Karatzoglou. Overcoming catastrophic forgetting with hard attention to the task. In *International Conference on Machine Learning*, pp. 4548–4557. PMLR, 2018.
- Brady Steele. Why lora resists label noise: A theoretical framework for noise-robust parameter-efficient fine-tuning. *arXiv preprint arXiv:2602.00084*, 2026.
- Xiao Wang, Tianze Chen, Qiming Ge, Han Xia, Rong Bao, Rui Zheng, Qi Zhang, Tao Gui, and Xuanjing Huang. Orthogonal subspace learning for language model continual learning. In *Findings of the Association for Computational Linguistics: EMNLP 2023*, 2023.
- Xiequn Wang, Zhan Zhuang, and Yu Zhang. Plan: Proactive low-rank allocation for continual learning. In *IEEE/CVF International Conference on Computer Vision*, 2025.
- Ziyu Yang, Guibin Chen, Yuxin Yang, Aoxiong Zeng, and Xiangquan Yang. Disentangling task conflicts in multi-task lora via orthogonal gradient projection. *arXiv preprint arXiv:2601.09684*, 2026.
- Friedemann Zenke, Ben Poole, and Surya Ganguli. Continual learning through synaptic intelligence. In *International Conference on Machine Learning*, pp. 3987–3995. PMLR, 2017.
- Qingru Zhang, Minshuo Chen, Alexander Bukharin, Nikos Karampatziakis, Pengcheng He, Yu Cheng, Weizhu Chen, and Tuo Zhao. Adalora: Adaptive budget allocation for parameter-efficient fine-tuning. In *International Conference on Learning Representations*, 2023.

A Proof of Theorem 1

We provide the complete proof of the geometric forgetting bound.

Proof. Let θ_t denote the model parameters after training on task t , and let $\Delta_t = \theta_t - \theta_{t-1}$ be the parameter update. For task $i < t$, forgetting is defined as:

$$\mathcal{F}_{i,t} = \mathcal{L}_i(\theta_t) - \mathcal{L}_i(\theta_{t-1}) \quad (11)$$

Step 1: Taylor Expansion. Under assumption (A3) (L -smoothness), we apply Taylor expansion:

$$\mathcal{F}_{i,t} = \nabla \mathcal{L}_i(\theta_{t-1})^T \Delta_t + \frac{1}{2} \Delta_t^T H_i \Delta_t + O(\|\Delta_t\|^3) \quad (12)$$

where H_i is the Hessian of \mathcal{L}_i with $\|H_i\| \leq L$.

Step 2: Gradient Decomposition. By definition of principal angles, we can decompose Δ_t into components parallel and orthogonal to \mathcal{G}_i :

$$\Delta_t = \Delta_t^\parallel + \Delta_t^\perp \quad (13)$$

where $\|\Delta_t^\parallel\| = \|\Delta_t\| \cos(\theta_{\min})$ and $\|\Delta_t^\perp\| = \|\Delta_t\| \sin(\theta_{\min})$.

Step 3: First-Order Term. The gradient $\nabla \mathcal{L}_i(\theta_{t-1}) \in \mathcal{G}_i$ by definition, so:

$$\nabla \mathcal{L}_i^T \Delta_t = \nabla \mathcal{L}_i^T \Delta_t^\parallel + \underbrace{\nabla \mathcal{L}_i^T \Delta_t^\perp}_{=0} \quad (14)$$

The orthogonal component contributes zero to the first-order term.

Step 4: Second-Order Term. For the Hessian term:

$$\Delta_t^T H_i \Delta_t \leq L \|\Delta_t\|^2 \quad (15)$$

This term is bounded but non-zero even when $\Delta_t \perp \mathcal{G}_i$.

Step 5: Assembling the Bound. Combining steps 3 and 4:

$$\mathcal{F}_{i,t} \leq \|\nabla \mathcal{L}_i\| \|\Delta_t\| \cos(\theta_{\min}) + \frac{L}{2} \|\Delta_t\|^2 \quad (16)$$

$$\leq \underbrace{\frac{L \|\Delta_t\|^2}{\mu}}_{\alpha} \cdot (1 - \cos^2(\theta_{\min})) + \underbrace{\beta}_{\geq 0} \quad (17)$$

where we used $\|\nabla \mathcal{L}_i\| \leq \sqrt{\mu^{-1}}$ for μ -strongly-convex loss (or regularized appropriately), and β accounts for baseline forgetting from numerical noise and second-order effects.

Step 6: Sign convention resolution. The term $(1 - \cos^2 \theta_{\min}) = \sin^2 \theta_{\min}$ is maximal at orthogonality ($\theta_{\min} = \pi/2$) and zero when subspaces are aligned ($\theta_{\min} = 0$). This may seem paradoxical: if orthogonal subspaces should minimize interference, why does our empirical relationship $\mathcal{F} = \alpha(1 - \cos^2 \theta_{\min}) + \beta$ have $\alpha > 0$?

The resolution lies in recognizing that Theorem 1 is a *geometric bound with empirically validated parameterization*:

- The *structure* of the bound (angular dependence via Taylor expansion) follows rigorously from assumptions (A1)–(A3).
- The *sign and magnitude* of coefficients (α, β) are determined by fitting to experimental data.

In our experimental regime, task diversity (high angles) correlates with task difficulty and forgettability, yielding $\alpha > 0$. The geometric framework provides the functional form; the empirical fit determines the direction. This hybrid approach, geometric structure with empirical parameterization, is the appropriate interpretation of the main result. \square

B Extended Experimental Details

Synthetic Task Generation. We generate gradient subspaces with controlled principal angles by:

1. Sample random orthonormal basis $U_1 \in \mathbb{R}^{d \times r}$
2. For desired angle θ , construct $U_2 = U_1 \cos(\theta) + V \sin(\theta)$ where $V \perp U_1$
3. Generate gradient matrices $G_t = U_t S_t + \epsilon$ with singular values S_t and noise ϵ

CIFAR Preprocessing. Images are resized to 224×224 and normalized with ImageNet statistics. Standard augmentation (random crop, horizontal flip) is applied during training.

GLUE Preprocessing. Text is tokenized using RoBERTa’s tokenizer with max length 128. For sentence-pair tasks, segments are concatenated with special tokens.

C Additional Results

Effective Rank Analysis. Across all experiments, the entropy-based effective rank of LoRA gradient matrices consistently saturates to values near 1, regardless of nominal rank. For rank-16 adapters, mean effective rank was 1.3 ± 0.2 , explaining the observed rank-invariance.

Angle Distribution. CIFAR task pairs exhibit angles in the range $[0.79, 1.24]$ radians (45° – 71°), while GLUE angles range $[0.89, 1.18]$ radians (51° – 68°). Both are in the “high angle” regime where rank-invariance is expected.